International Journal of Concrete Structures and Materials
Vol.7, No.1, pp.71–78, March 2013
DOI 10.1007/s40069-013-0033-4
ISSN 1976-0485 / eISSN 2234-1315

Shear Cracking of Prestressed Girders with High Strength Concrete

Emad L. Labib, Y. L. Mo*, and Thomas T. C. Hsu

(Received December 25, 2012, Accepted February 11, 2013)

Abstract: Prestressed concrete (PC) is the predominant material in highway bridge construction. The use of high-strength concrete has gained wide acceptance in the PC industry. The main target in the highway industry is to increase the durability and the life-span of bridges. Cracking of elements is one aspect which affects durability. Recently, nine 7.62 meter long PC I-beams made with different concrete strength were designed according to a simple, semi-empirical equation developed at the University of Houston (UH) (Laskar et al., ACI Journal 107(3): 330–339, 2010). The UH Method is a function of shear span-to-depth ratio (a/d), concrete strength $\sqrt{f'_c}$, web area $b_w d$, and amount of transverse steel. Based on testing these girders, the shear cracking strength of girders with different concrete strength and different shear span-to-depth ratio was investigated and compared to the available approaches in current codes such as ACI 318-11 (2011) and AASHTO LRFD Specifications (2010).

Keywords: shear cracks, high strength concrete, prestressed beams, full-scale tests.

1. Introduction

The use of high strength concrete (HSC, i.e. concrete compressive strength $f'_c > 55$ MPa) has gained wide acceptance in the PC industry. Standardization in the design and manufacturing of the precast bridges has been optimized. Bridge superstructure elements such as the PC I-beams, double tee and box beams are generally plant-produced precast and PC products inheriting the advantages of durability, economy, low maintenance and assured quality. The most commonly used precast/PC beam for short-to-medium-spans is the I-beam. An I-beam consists of a top and a bottom flanges with a slender web joining the flanges. The bottom flange and some portion of the web-bottom are reinforced with prestressing strands (tendons); thus the bottom and top flanges build up the flexural strength. The web is reinforced with vertical/transverse deformed reinforcing bars (rebars), referred to as stirrups, which contributes towards the shear strength of the beam.

In the design of PC girders, an adequate margin of safety must be provided against both flexure and shear cracking under service load. Although cracking does not mean a structural failure, in the long term, cracking affects the durability of the structural element. It increases the environmental effects on the embedded steel. Moreover, cracks in general looks uncomfortable for public. Therefore, one of the most important criteria in designing concrete structure is to prevent cracking under the act of the different loads.

Department of Civil and Environmental Engineering, University of Houston, Houston, TX 77204, USA.
*Corresponding Author; E-mail: yilungmo@egr.uh.edu

Cracking stress of a structural element in shear, which is the concern of this paper, does not depend on the amount of transverse steel. It depends only on the tensile strength of concrete. Most the current provisions, such as ACI Codes and AASHTO LRFD Specifications, calculate the tensile strength as a function in the concrete compressive strength f'_c. Rizkalla et al. (2009) conducted an experimental program to study material properties of PC members. Based on comparing the experimental results with AASHTO LRFD specifications, they found that the currently specified modulus of rupture might not be satisfied for high strength concrete. Perera and Mutsuyoshi (2011), concluded based on testing high strength concrete tension members that the average tensile strength for different concrete strength even higher than 100 MPa were between $0.32\sqrt{f'_c}$ and $0.37\sqrt{f'_c}$.

In general, the current code provisions were driven for normal concrete $\left(f'_c < 55\,\text{MPa}\right)$. The primary focus of this paper is to compare the current codes provisions of calculating the tensile strength in the web at shear cracking to that obtained from the experimental program presented later. The tested girders had different concrete compressive strengths and different transverse reinforcement ratios. The girders were also loaded using different shear span-to-depth ratios as will be discussed later.

2. Experimental Program

Nine girders were designed, cast, and tested to investigate the shear cracking strength of the web of PC I-girders. Girders had an effective depth of 611 mm and a web thickness of 76 mm. Girders had different concrete compressive strength. Because it is very difficult to measure stresses during experiments, an indirect method was used. The method depends on finding the stresses by knowing strains and the modulus of elasticity of concrete. As it will be discussed later, strains in the web was measured at each side by using a complete rosette of ten linear variable displacement transformers (LVDT). The modulus of elasticity for the different concrete was found by testing standard cylinders 152 × 304 mm. The compressive strain along the cylinders' longitudinal axis was measured using 203 mm extensometer installed at the middle of the tested cylinders according to ASTM-C469 (2002).

3. Test Girders

TxDOT currently uses Tx-series of PC girders for highway bridge construction. Tx-series girders have a web thickness of 178 mm and depths ranging from 711 to 1,829 mm. Typically Tx-series girders have a top slab with a thickness 203 mm and the minimum spacing between girders is 2,032 mm. In this research an internal Tx54 was considered with a top slab 2,032 mm wide. The resulting girder cross section was scaled down to 43 % to form the modified Tx28 girder, Fig. 1, which was used in seven of the tested girders. The other two girders had the same web thickness and effective depth, Fig. 2. Their bottom flange had a higher depth by one inch to accommodate the additional longitudinal reinforcement required to increase the flexure capacity and ensure having a shear failure at the ultimate load. Also, their top flange had a reduced width equals to the width of the real top flange scaled down by the same ratio to allow flexure shear failure to happen at the ultimate load. These two modifications in the cross section should not have any effect on the shear cracking strength of the web.

In total nine full-scale modified Tx28 girders with a length of 7.62 m were tested at UH under this research work. The nine girders were divided into three groups based on the average compressive strength. Two "Group A" Girders (A1 and A2) with concrete compressive strength of $f'_c \cong 48.26\,\text{MPa}$; four "Group F" Girders (F1–F4) with concrete compressive strength of $f'_c \cong 89.63\,\text{MPa}$; and three "Group C" Girders (C2–C4) with concrete compressive strength of $f'_c \cong 110.32\,\text{MPa}$ were investigated in this research. Table 1 shows the concrete mix proportions used for casting the girders in these groups. Texas Concrete Company produced the first two concrete mixes for Groups A and F at their precast plant in Victoria, Texas. Flexicore of Texas precast plant in Houston produced the concrete mix for Group C.

Several cylinders 150 × 300 mm were cast at the same time with each girder. The concrete was placed into each cylinder in three layers. Each layer was tapped with round rod 25 times. Then, cylinders was initially cured by keeping them covered under the same conditions as their girders.

Groups A and F girders had 14 seven-wire, low-relaxation prestressed straight tendons with a diameter of 13 mm, as a flexural reinforcement in the bottom flange. Group C girders had 14 seven-wire, low-relaxation prestressed straight tendons with a diameter of 13 mm oversized to increase the bending moment capacity ensuring shear failure of the girders. The prestressing tendons had a nominal tensile strength of 1,862 MPa. The locations of the prestressing tendons and different types of reinforcing steel in the tested girders are shown in Figs. 1 and 2.

In this paper, shear cracking is investigated using different shear span-to-depth ratios in each group of girders. Girders A1, F1, F3, and C3 were loaded using shear span-to-depth ratio of 1.77. Girders A2, F2, C2, and C4 were loaded using shear span-to-depth ratio of 3.00. Only girder F4 was loaded using shear span-to-depth ratio of 2.25. The locations of the applied actuator loads and support reactions are shown in Fig. 3.

The transverse reinforcement (stirrups) of the tested girders had been designed according to University of Houston design method developed recently by Laskar et al. (2010). In this design method the balanced shear strength, where the concrete crushes and steel yields simultaneously, is a function of the web dimensions and the used concrete compressive strength and is calculated as:

$$V_{u,\,\text{balanced}} = 1.5 b_w d \sqrt{f'_c(\text{MPa})}$$

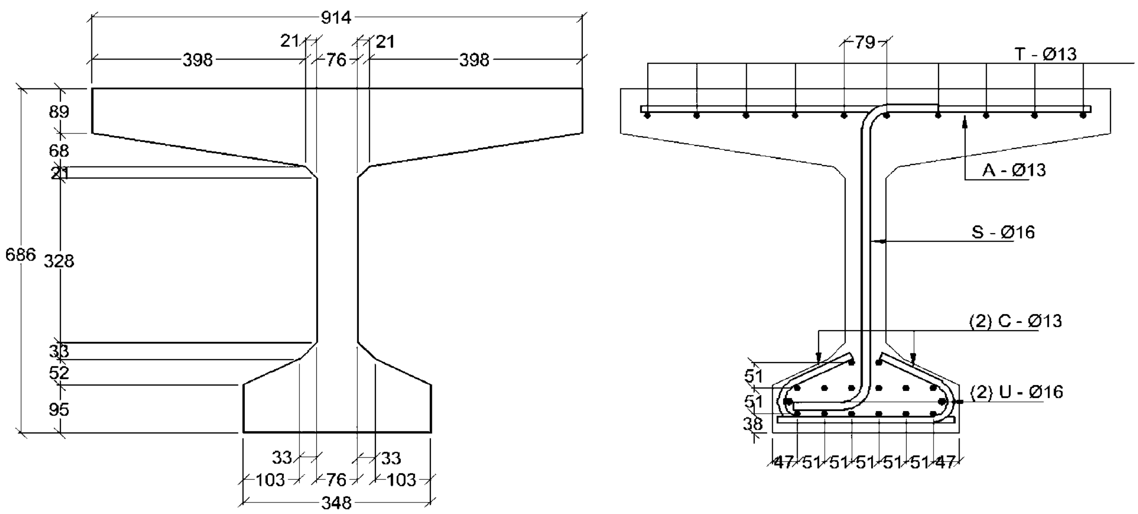

Fig. 1 Cross-section and reinforcement details for modified Tx28 Girders A1, A2, F1 to F4 and C3 (All dimensions are in mm).

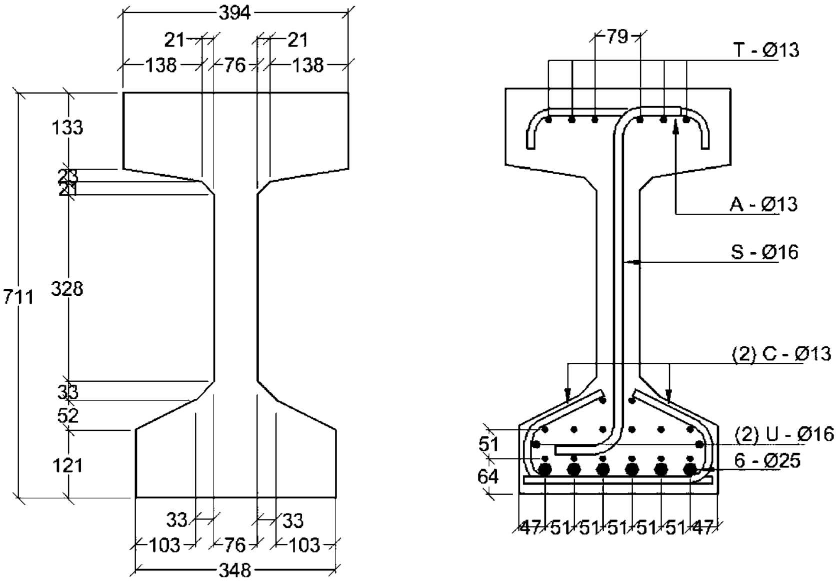

Fig. 2 Cross-section and reinforcement details for modified Tx28 Girders C2 and C4 (All dimensions are in mm).

Table 1 Concrete mix proportions used for casting girders.

Materials kg/m^3	Group A	Group F	Group C
Cement type-III	218	308	415
Fly ash type-F	89	147	119
Cementitious content	307	455	534
Fine aggregate	685	685	634
Coarse aggregate	1304[a]	1125[a]	1304[b]
Coarse agg./fineagg. ratio	1.91	1.64	2.06
Water	107	136	142
Water/cement ratio	0.49	0.43	0.34
Water/cementitious materials ratio	0.35	0.30	0.27
Superplasticizer (mL/100 kg)	–	624[c]	832[d]
Retarder (mL/100 kg)	–	65	260
Slump (cm)	16.5	21.6	26.7
Actual average strength (MPa)	48.3[e]	89.6[e]	110.3[e]

[a] 20 mm rounded river-bed.

[b] 20 mm dolomite, burnet, Texas.

[c] BASF (Glenium7700).

[d] Sika (ViscoCrete2110).

[e] At the testing day.

The shear force resisted by the concrete (concrete contribution to shear V_c) was found to be also a function of the web dimensions, concrete compressive strength and the shear span-to-depth ratio. The concrete contribution can be calculated as:

$$V_c = \frac{1.17}{(a/d)^{0.7}}\sqrt{\mathrm{f}'_\mathrm{c}(\mathrm{MPa})}b_w d \leq 10\sqrt{\mathrm{f}'_\mathrm{c}}b_w d$$

At balanced design the shear force resisted by the transverse steel (steel contribution to shear V_s) is estimated as

$$V_s = V_{u,\,\mathrm{balanced}} - V_c$$

The steel contribution, V_s, must be based on the observed failure shear crack. For design, the failure crack can be assumed to be inclined at a 45$^\mathrm{o}$ angle, similar to the ACI Code. In Laskar et al. (2010), a more realistic concept of seeking a path of minimum shear resistance among a series of individual stirrups is used. The minimum number of stirrups intersecting the minimum shear resistance line at 45$^\mathrm{o}$ is taken as $[(d/s) - 1]$. Thus,

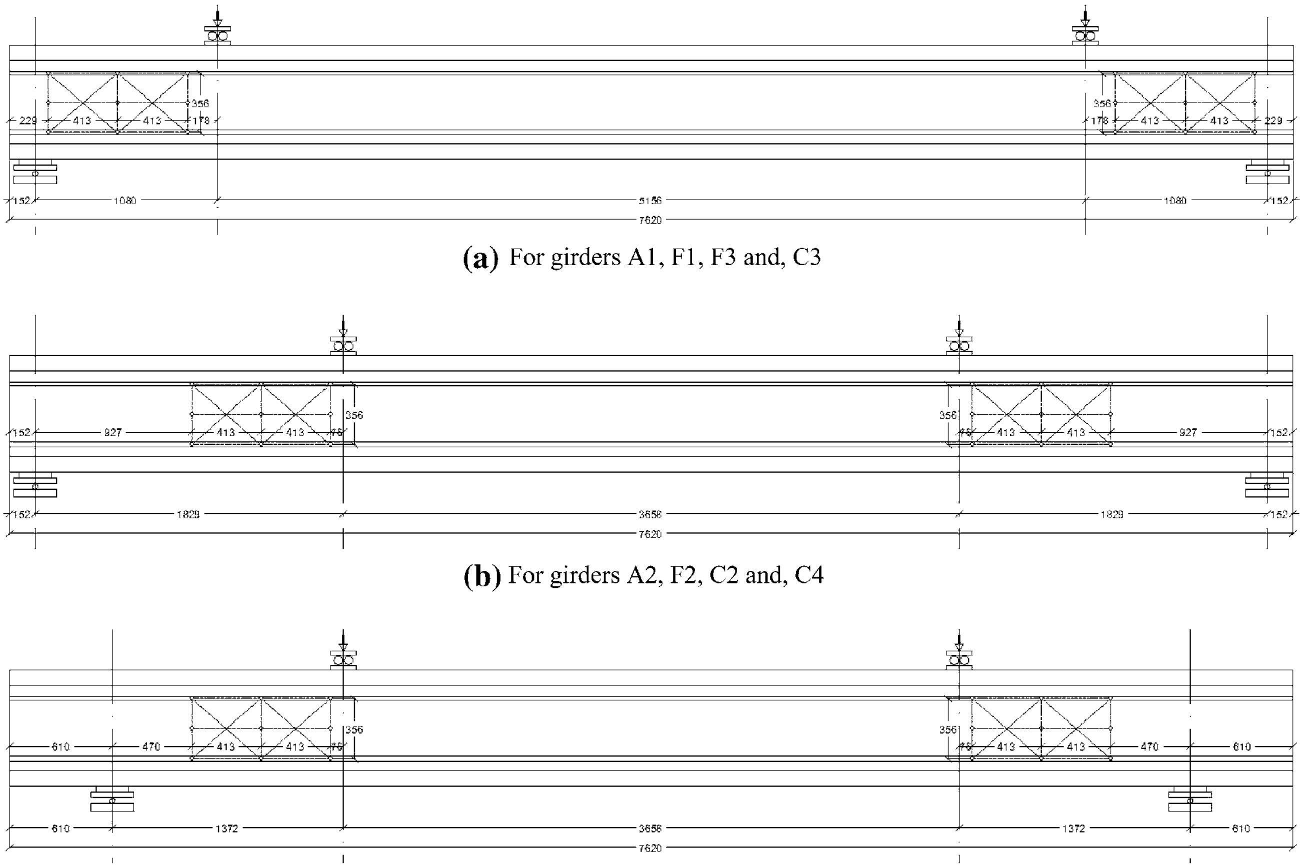

(a) For girders A1, F1, F3 and, C3

(b) For girders A2, F2, C2 and, C4

(c) For girder F4

Fig. 3 Locations of applied actuator loads and support reactions. **a** For girders A1, F1, F3 and, C3. **b** For girders A2, F2, C2 and, C4. **c** For girder F4 (All dimensions are in mm).

Table 2 Reinforcement Details for Modified Tx28 Girders (All dimensions are in mm).

Girder	Tendons		Mild steel reinforcement								
	Nos.	Dia.	Transverse Steel (ϕ16) “S”-rebar		Top flange flexural steel (ϕ13)				Bottom flange flexural steel		
			Sp.	Ratio (%)	Longitudinal direction “T”-rebar		Lateral direction “A”-rebar		Extra flexural steel	Confinement steel (ϕ13) “C”-rebar	
					Nos.	Sp.	Nos.	Sp.		Nos.	Sp.
A1	14	12.7	149	1.76	10	89	26	298	–	106	149
A2	14	12.7	114	2.30	10	89	34	229	–	138	114
F1	14	12.7	140	1.88	10	89	28	279	–	114	140
F2	14	12.7	102	2.58	10	89	38	203	–	154	102
F3	14	12.7	108	2.43	10	89	36	216	–	146	108
F4	14	12.7	79	3.31	10	89	32	248	–	196	83
C2	14	12.7[a]	83	3.18	6	38	32	248	6 ϕ 25	96	165
C3	14	12.7[a]	76	3.44	10	89	27	305	–	100	152
C4	14	12.7[a]	64	4.13	6	38	30	191	6 ϕ 25	120	127

Nos. total number of rebars.

[a] Oversize Sp.—spacing c/c (mm).

$$V_s = A_v f_y \left(\frac{d}{s} - 1 \right)$$

The web of all test girders was reinforced in the transverse direction with one legged stirrups called S rebars, that are fabricated using 16 mm diameter mild steel bars with a nominal tensile strength 413 MPa. The spacing between stirrups was justified either to have crushing of concrete struts and yielding of steel simultaneously at the ultimate load (balanced design), or to have crushing of concrete struts prior to yielding of steel (over-reinforced design). Girders A1, A2, F1, F2, and C2 were designed for a balanced cross sections while Girders F3, F4, C3, and C4 were designed to have over-reinforced cross sections. In addition to the transverse direction reinforcement, 16 mm diameter bars were used for U rebars that were designed to resist the end zone bearing, spalling, and bursting stresses. For C, A, and T rebars, 13 mm diameter bar was used; whereas C rebars were designed to confine concrete and act as secondary reinforcements in the bottom flange. A and T rebars were designed to be the lateral and longitudinal flexural reinforcement in the top flange. Table 2 presents the reinforcement details for all the tested girders.

4. Test Set Up

The girders were subjected to vertical loading up to their maximum shear capacity in a specially built steel loading frame (Fig. 4). Two of the four actuators (actuator B and actuator C) attached to a vertical steel frame and were used to apply the vertical loads on the girders. Each of the two actuators had a capacity of 1,423 KN in compression. Actuator frames B and C were installed on the north and south ends of the girder, respectively. These two actuator frames were placed on top of two WF18 × 97 girders, bolted securely to the strong floor. The two WF18 × 97 girders were 6.1 m long and spaced at 2,210 mm center to center.

The girder was positioned in the middle of this spacing width on top of two load cells placed at the north and south ends. The load cells of 2,224 KN capacity were placed on top of the steel pedestals fixed to the strong floor. On top of the load cells, bearing plates to support the girders were placed with a roller on the north end and a hinge on the south end, thus allowing the girder to rotate freely at the supports and to expand freely along its length. The actuators were provided with bracings for their lateral stability.

Actuator loads were applied through a roller assembly consisting of two 152 × 305 × 51 mm thick hardened steel bearing plates and two hardened steel rollers of 51 mm diameter and 305 mm in length. This ensured uniform and frictionless load transfer from actuators to the girder surface. The bearing plates and rollers were heat-treated to maximum possible hardness, to minimize local deformations. Lead sheets were used between the load bearing plates and girder surface to aid in uniform loading. The MTS "MultiFlex" System precisely controlled the applied loads and displacements through the actuators. Each girder was first loaded using Actuators B and C under a load-control mode at a rate of

Fig. 4 Test set up for girders.

Fig. 5 Test set up for finding modulus of elasticity.

9 KN/min. As soon as the slope of load versus displacement curve for girder being tested dropped, the actuator control-mode was switched to a displacement-control at a rate of 5 mm/h until shear failure occurred at either end of the girder. The displacement-control mode was essential in capturing the ductility or brittleness behavior of the girder failing in shear.

The day after the girder was tested, the cylinders cast previously simultaneously with each girder using the same concrete were tested to get the concrete compressive strength for the tested girder. Some cylinders were tested to get the modulus of elasticity according to ASTM-C469 (2002) Fig. 5, using the facility available at the University of Houston. The used dial gauge had a precision of 0.0025 mm.

5. Instrumentations

To measure the average or smeared strain in concrete within the expected failure region of the girder web, a set of 10 LVDTs were used in a rosette formation on the east and west faces and either ends of the girder (Fig. 6).

Strains measured by the above discussed sensors and the applied loads by actuators as well as the shear forces at both ends of each girder measured by actuators and load cells

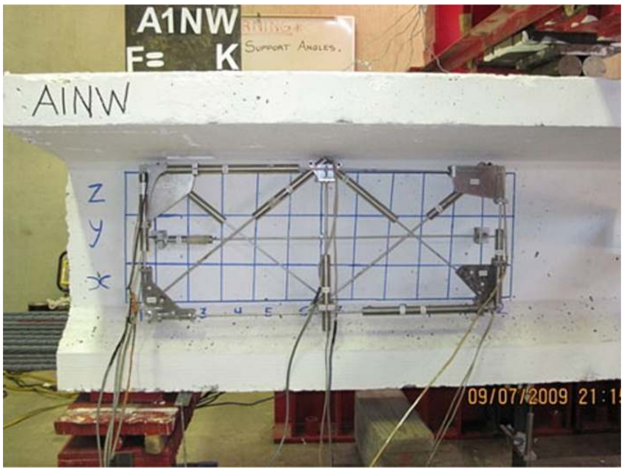

Fig. 6 LVDT rosette installed on girders.

respectively were monitored continuously and stored by the HBM "Spider-8" Data Acquisition System. Shear and flexure cracks formed on the girder during the load test regularly were marked on the grid. Shear crack widths were measured at different load intervals using a hand-held microscope having a 0.0254 mm measuring precision.

6. Test Results and Discussion

6.1 Experimental Modulus of Elasticity

Table 3 summarizes the test variables, the experimental modulus of elasticity and the estimated tensile strength. Each girder had two estimated values for tensile strength at both the north and the south ends except girders A2 and C4.

Girder A2 was loaded using shear span-to-depth ration of 3.00. The LVDTs rosette was installed next to the loading points (actuators) as can be seen in Fig. 3. During the test, the north LVDT rosette missed measuring the tensile strains at the location of first shear crack which appeared out of the studied zone.

At the beginning of testing girder C4, the south actuator had a controlling problem which resulted in applying a huge sudden load which let the south end cracked before the starting of the test. Therefore, the tensile strains measured during the test at the south end did not considered in calculating the tensile stresses of the girder because they are not virgin readings.

Because the concrete is well known for its non-linear stress–strain curves. The initial stiffness of the stress–strain curve which represents the modulus of elasticity E_c was evaluated within the linear segment at the beginning of the stress–strain relationships. This linear segment is taken till the stress of 45 % of the ultimate compressive strength according to ACI 318-11 (2011). Vogel and Svecova (2012) took the initial stiffness till stress equals to 40 % of the ultimate strength of the tested cylinder.

ACI 318-11 (2011) and AASHTO LRFD (2010) have a simple equation for calculating the elastic modulus of concrete which was derived for concrete compressive strength up to 42 MPa. This equation calculates the modulus of elasticity as a function of the density and the compressive strength of the concrete as

Table 3 Test variables and tensile strength at shear cracking of girders.

Beam I.D.	a/d	f'_c (MPa)	(ρ %)	E (MPa)	f_t (MPa)	
A1	1.77	48.28	1.76	29,968	North	4.27
					South	3.60
A2	3.00	49.66	2.30	30,295	North	–
					South	3.67
F1	1.77	91.03	1.88	38,577	North	4.42
					South	4.65
F2	3.00	89.66	2.58	38,336	North	3.8
					South	4.68
F3	1.77	91.72	2.43	38,697	North	3.48
					South	3.64
F4	2.25	90.34	3.31	38,457	North	4.61
					South	6.06
C2	3.00	103.45	3.18	40,668	North	3.46
					South	4.07
C3	1.77	116.55	3.44	42,742	North	5.13
					South	5.00
C4	3.00	105.52	4.13	41,004	North	4.08
					South	–

$$E_c = 0.043 w_c^{1.5} \sqrt{f'_c}(\mathrm{MPa})$$

which for the normal weight concrete can be simplified as

$$E_c = 4700 \sqrt{f'_c}(\mathrm{MPa})$$

The elastic modulus of concrete with compressive strength higher than 42 MPa evaluated experimentally by Kaar et al. (1978), Perenchio et al. (1978) Carrasquiho et al. (1982), Martinez et al. (1982) was found to better fit the ACI 363R-92 (1997) formula, which calculates the modulus of elasticity as

$$E_c = 3320 \sqrt{f'_c}(\mathrm{MPa}) + 6900$$

Figure 7 shows the modulus of elasticity of the tested girders concrete compared to the previous two approaches. This comparison shows that the modulus of elasticity found experimentally in this research work is closer to the expression given in ACI 318-11 (2011) and AASHTO LRFD (2010) for the normal weight concrete. Based on the current research results, this approach was confirmed to be applicable to concrete strength up to 117 MPa.

6.2 Tensile Strain in Concrete at Shear cracking

According to the ACI 318-11 (2011), the shear cracks should start to appear in the web of prestressed I-girders if the principle tensile stress at the location of expected shear cracks exceeds $0.33\sqrt{f'_c}(\mathrm{MPa})$. Tamai et al. (1987) used $0.31\sqrt{f'_c}(\mathrm{MPa})$ as a limit for the tensile strength causing cracks in concrete. This approach was later used by Belarbi and Hsu (1995) to establish the smeared concept of smeared cracked of concrete under shear. National Cooperative Highway Research Program has tested ten full scale prestressed girders at University of Illinois (NCHRP 2007). They loaded the girders with a uniform distributed load till failure. They observed that the first crack was always a web shear crack. In most the cases this first web shear crack appeared at higher load than the cracking load V_{cw} specified in AASHTO Standard Specifications (2002). This

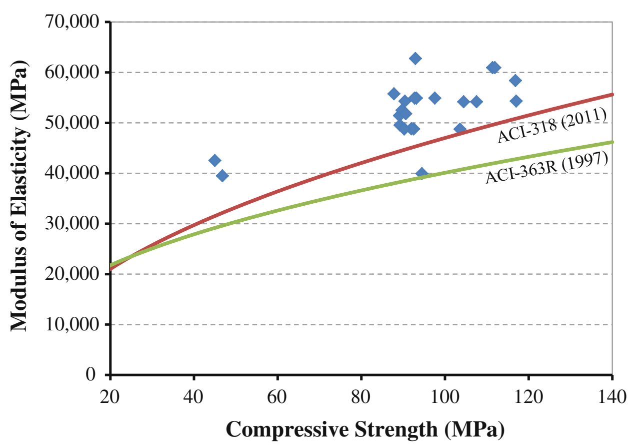

Fig. 7 Modulus of elasticity of current girders compared to the ACI 318-11 (2011) and ACI-363R-92 (1997) approaches.

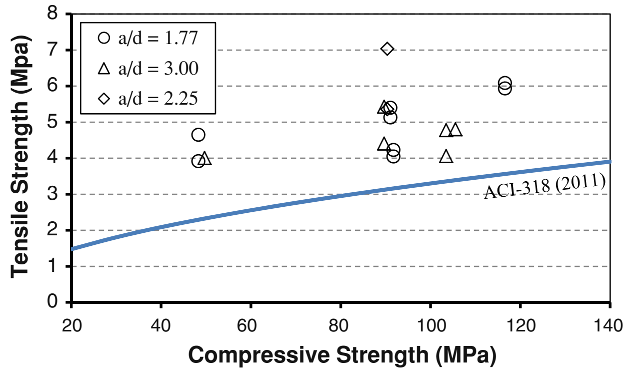

Fig. 8 Tensile strength at shear cracking versus concrete compressive strength.

experimental program could not evaluate the cracking load at different shear span-to-depth ratios because of using a uniform distributed load.

In this paper, the ACI 318-11 (2011) approach will be validated for different concrete strength. Therefore, the cracking tensile stresses of the test girders need to be evaluated. The easiest and the most accurate way to evaluate stresses in such specimens is to measure the corresponding strains, and by knowing the modulus of elasticity of used material, stresses can be evaluated.

Thus, the tensile strain across shear cracks was measured at two adjacent locations in the studied zone at both sides of each girder end. Thus, the average cracking strain through the entire studied zone for each end was considered as the average of these four measured strains. Since ACI 318-11 (2011) approach for the modulus of elasticity was proved using the current study data to be applicable for higher strength of concrete, it will be used to estimate the tensile stress causes the web shear cracks in the studied girders. The estimated tensile strength of each end of test girders is compared to the minimum principle tensile strength $\left(0.33\sqrt{f'_c}(\mathrm{MPa})\right)$ according to ACI 318-11 (2011) in Fig. 8. This comparison confirms that this estimation still valid for concrete with compressive strength up to 117 MPa.

The ultimate shear strength of the PC girders is known to be strongly affected by the shear span-to-depth ratio. This was obviously concluded from the experimental tests done before by many researchers such as Lyngberg (1976), Elzanaty et al. (1986), Robertson and Durrani (1987), Kaufman and Ramirez (1988), Shahawy and Batchelor (1996), and recently by Laskar et al. (2010). From Fig. 8 it can be concluded that the tensile strength causing shear cracks is not affected by the shear span-to-depth ratio used in loading the girders. It can be seen that the measured tensile strength at cracking using different shear span-to-depth ratios is comparable for the same concrete strength.

7. Conclusions

1. The ACI 318-11 (2011) approach for calculating the modulus of elasticity is still valid for high strength concrete up to 117 MPa.

2. The experimental results from this study shows that the ACI 318-11 (2011) approach of calculating the shear cracking strength of PC girders is still valid for high-strength concrete up to 117 MPa.
3. The shear cracking strength of PC girders is not affected by the shear span-to-depth ratio or the amount of transverse steel.

Acknowledgments

The research presented in this paper is financially supported by Texas Department of Transportation. The research findings presented in this paper are those from the authors, and they are not necessary to express the sponsor's opinion.

Open Access

References

AASHTO. (2002). *Standard specifications for highway bridges* (17th ed.). Washington, DC: American Association of State Highway and Transportation Officials (AASHTO).

AASHTO. (2010). *AASHTO LRFD bridge design specifications* (4th ed.). Washington, DC: American Association of State Highway and Transportation Officials (AASHTO).

ACI 363R-92. (1997). *State-of-the-art report on high strength concrete*. ACI Committee Report, pp. 55.

ACI 318-11. (2011). *Building code requirements for structural concrete*. American Concrete Institute, Farmington Hills, MI: American Concrete Institute.

ASTM-C469. (2002). *Static modulus of elasticity and Poisson's ratio of concrete in compression*. West Conshohocken, PA: ASTM International.

Belarbi, A., & Hsu, T. T. C. (1995). Constitutive laws of softened concrete in biaxial tension–compression. *ACI Structural Journal, 92*(5), 562–573.

Carrasquiho, R. L., Nilson, A. H., & Slate, F. O. (1982). Properties of High Strength Concrete Subjected to Short-Term Loads. *ACI Journal*, Proceedings V. 78, No. 3, May–June 1981, pp. 171–178, and Discussion, Proceedings V. 79, No. 2, Mar–Apr. 1982, pp. 162–163.

Elzanaty, A. H., Nilson, A. H., & Slate, F. O. (1986). Shear capacity of prestressed concrete girders using high-strength concrete. *ACI Journal, 83*(3), 359–368.

Kaar, P. H., Hanson, N. W., & Capell, H. T. (1978). *Stress-strain characteristics of high-strength concrete*. Douglas McHenry International Symposium on Concrete and Concrete Structures, SP-55, American Concrete Institute, Detroit, 1978, pp. 161–185. Also, Research and Development Bulletin No. 051.01D, Portland Cement Association.

Kaufman, M. K., & Ramirez, J. A. (1988). Re-evaluation of ultimate shear behavior of high-strength concrete prestressed I-girders. *ACI Structural Journal, 85*(3), 295–303.

Laskar, A., Hsu, T. T. C., & Mo, Y. L. (2010). Shear strength of prestressed concrete beams part 1: Experiments and shear design equations. *ACI Journal, 107*(3), 330–339.

Lyngberg, B. S. (1976). Ultimate shear resistance of partially prestressed reinforced concrete I-beams. *ACI Journal, 73*(4), 214–222.

Martinez, S., NiIson, A. H., & Slate, F. O. (1982). *Spirally-reinforced high-strength concrete columns*. Research Report No. 82–10, Department of Structural Engineering, Cornell University, Ithaca, NY.

NCHRP 579. (2007). *Application of LRFD bridge design specifications to high-strength structural concrete: Shear provisions*. NCHRP Report 579, Transportation Research Board, sponsored by ASSHTO and FHWA.

Perenchio, W. F., & Khieger, P. (1978). *Some physical properties of high strength concrete*, Research and Development Bulletin No. RD056.01T, Portland Cement Association, Skokie, pp. 7.

Perera, S. V. T. J., & Mutsuyoshi, H. (2011). Tension stiffening behavior of high-strength concrete tension members. *Annual Research Journal of SLSAJ, 11*, 10–18.

Rizkalla, S., Zia, P., Mirmiran, A., Russell, H. G., & Mast, R. (2009). Proposal for concrete strength up to 124 MPa for bridge design. Journal of the Transportation Research Record, No. 2131, pp. 59–67.

Robertson, I. N., & Durrani, A. J. (1987). Shear strength of prestressed concrete T girders with welded wire fabric as shear reinforcement. *PCI Journal, 32*(3), 46–61.

Shahawy, M. A., & Batchelor, B. (1996). Shear behavior of full-scale prestressed concrete girders: Comparison between AASTHO specifications and LRFD code. *PCI Journal, Precast/Prestressed Concrete Institute, 41*(3), 48–62.

Tamai, S., Shima, H., Izumo, J., & Okamura, H. (1987). *Average stress–strain relationship in post yield range of steel bar in concrete*. Concrete Library of JSCE, No. 11, June 1988, pp. 117–129. (Translation from Proceedings of JSCE, No. 378/Vol. 6, Feb 1987).

Vogel, H. M., & Svecova, D. (2012). Evaluation of elastic modulus for high-strength concrete. *ACI Materials Journal, 109*(M29), 313–322.